Metal-Free ATRP Catalyzed by Visible Light in Continuous Flow

Nassim El Achi, Youssef Bakkour, Wissal Adhami, Julien Molina, Maël Penhoat, Nathalie Azaroual, Laetitia Chausset-Boissarie, Christian Rolando

Metal Free ATRP Catalyzed by Visible Light in Continuous Flow

Nassim El Achi,[1] Youssef Bakkour,[2] Wissal Adhami,[1,2] Julien Molina,[1] Maël Penhoat,[1] Nathalie Azaroual,[3] Laëtitia Chausset-Boissarie,[1] and Christian Rolando[1]*

[1]Université de Lille, USR CNRS 3290, MSAP ‘ Miniaturisation pour la Synthèse l'Analyse et la Protéomique ‘, F-59000 Lille, France

[2]Laboratory of Applied Chemistry, Faculty of Sciences III, Lebanese University, PO Box 826, Tripoli, Lebanon

[3] Université de Lille, EA 7365, GRITA ‘Groupe de Recherche sur les formes Injectables et les Technologies Associées’, Laboratoire de Physique et d'Application RMN, F-59000 Lille, France

*** Correspondence:**
Christian Rolando
christian.rolando@univ-lille.fr

Keywords: ATRP, continuous flow, visible light, Eosin Y, DOSY NMR

Abstract

ATRP of methyl methacrylate catalyzed by Eosin Y, an inexpensive and an environmental benign dye, was performed in a continuous flow reactor made of FEP tubing and irradiated by visible light green LEDs. The reaction under flow conditions was significantly more rapid and controlled compared to that in batch giving 90% of polymerization after only 3 h of irradiation. The formed polymers in flow have M_n measured by GPC and DOSY NMR in accordance with the theoretical values and show low dispersities ($Đ$ < 1.5). The livingness of the polymers has been confirmed by LEDs on and LEDs off experiments and by the synthesis of block copolymers. The protocol described herein serves as a “proof of concept” of using Eoin Y as a photocatalyst for controlled polymerization and of using 1D and 2D- NMR for polymer characterization. The protocol could be replicated in the future for other reversible-deactivation radical polymerizations.

1 Introduction

During the last decade, much attention has been given to reversible deactivation radical polymerization (RDRP) in polymer and material chemistry as it is considered a reliable technique for the production of controlled/living polymers offering wide range of methods like nitroxide-mediated radical polymerization (NMP), reversible addition-fragmentation chain transfer (RAFT), variations of organometallic-mediated polymerizations (OMBP), and atom transfer radical polymerization (ATRP) (Gao and Matyjaszewski, 2006;Chmielarz et al., 2017;Fantin et al., 2017).

ATRP has become widely employed due to its remarkable performance in the synthesis of polymers of well-defined chemical composition and complex architecture (Matyjaszewski and Xia, 2001;Ouchi et al., 2008;Matyjaszewski and Tsarevsky, 2009;Ouchi et al., 2009;Matyjaszewski, 2012;Matyjaszewski and Tsarevsky, 2014;Boyer et al., 2016;Ribelli et al., 2019).

In an aim to develop more sustainable and visible light mediated ATRP (Corrigan et al., 2019), researchers have developed photoredox catalytic systems using catalysts like copper (Cu) (Tasdelen

et al., 2011;Konkolewicz et al., 2012;Mosnacek and Ilcikova, 2012;Anastasaki et al., 2014;Ribelli et al., 2014;Yang et al., 2015), cyclometallated Iridium (Ir) (Fors and Hawker, 2012;Ma et al., 2014;Treat et al., 2014a;Xu et al., 2014;Ma et al., 2015) or Ruthenium (Ru) (Zhang et al., 2011;Alfredo et al., 2012;Priyadarshani et al., 2013).

Despite their effectiveness, metal contamination limits their interest for biomedical and electronic applications. significant efforts has therefore been dedicated to develop photoredox metal free ATRP (Chen et al., 2016;Pan et al., 2016b;Hu et al., 2017;Ryan et al., 2017;Discekici et al., 2018). Pioneering work by Hawker group demonstrated that 10-phenylphenothiazine (PTH) can be an effective organic photoredox catalyst for the polymerization of methacrylates under ultraviolet irradiation (Treat et al., 2014b). Subsequently, the group of Matyjaszewski has extended the methodology to polyacrylonitrile synthesis (Pan et al., 2015).

More importantly, a photoredox ATRP mediated by visible light using organic photoredox catalyst like perylene and fluorescein has been reported with the latter requiring prolonged irradiation times (Miyake and Theriot, 2014) (Liu et al., 2016). However, some drawbacks are still present like low initiator efficiency that leads to polymers of elevated masses and dispersity (*Đ*).

To address this challenge {Discekici, 2018 #71}, the group of Miyake introduced diphenyl dihydrophenazine derivatives as metal free photocatalysts (Theriot et al., 2016;Ryan et al., 2017) and recently dimethyl dihydroacridines {Buss, 2020 #79}. Yagci group also recently reported a metal-free photoinduced ATRP using Eosin Y (Figure 1) (Kutahya et al., 2016;Yilmaz and Yagci, 2018). Their work gave promising results but with some challenges regarding dispersity and reaction time. To overcome these issues, continuous photoflow reactor can be used since the short optical lengths of flow microreactors can significantly improve sample irradiation and heat and mass transfer that allow the use of more concentrated photoinitiators (Elliott et al., 2014;Garlets et al., 2014;Su et al., 2014;Cambié et al., 2016). Consequently, flow chemistry has recently been used in polymer synthesis since it provides improved initiator efficiency and better-controlled polymers of narrow dispersity compared to classical batch processes (Tonhauser et al., 2012;Chatani et al., 2014;Myers et al., 2014;Reis et al., 2020). However, this field is not widely studied with only few articles addressing ATRP in flow (Wenn et al., 2014;Melker et al., 2015;Hu et al., 2016;Corrigan et al., 2017;Ramakers et al., 2017;Rubens et al., 2017;Zhang et al., 2019); including those using non-commercially available photoredox catalysts (Ramsey et al., 2017;Ryan et al., 2017;Buss and Miyake, 2018).

Since our research group focuses on performing wide range of photocatalytic reactions in flow, we herein present the use of Eosin Y as a photocatalyst for ATRP in flow using visible light. The study falls in the category of "proof of concept" where it aims to determine whether using this cheap and commercially available photocatalyst for ATRP in flow would provide better results than those obtained in batch by Yagci group (Kutahya et al., 2016;Yilmaz and Yagci, 2018); and therefore can be used for other reversible-deactivation radical polymerizations.

2 Materials

2.1 Chemicals

Tris(2,2′-bipyridyl)ruthenium(II) chloride hexahydrate ($Ru(bpy)_3Cl_2.6H_2O$, 99.95%) was purchased from Strem Chemicals Inc. (Newbury port, MA, USA), Eosin Y from Alfa Aesar (Haverhill, MA, USA) and copper (II) bromide ($CuBr_2$, 99%) and all other reagents were purchased from Sigma-

Aldrich (St. Louis, MO, USA). All solvents were purchased dry from Sigma-Aldrich (St. Louis, MO, USA) and used as received unless otherwise stated.

Anhydrous *N*,*N*-diisopropylethylamine (*i*-Pr_2NEt, ≥ 99%) was further distilled over KOH and stored in dark under argon before usage. Methyl methacrylate (99%) was passed over alumina to remove the hydroquinone stabilizer immediately prior to use.

2.2 Flow System

The lab designed microreactor is composed of FEP (fluorinated ethylene propylene) tubing (i.d. 800 µm, length 1.20 m, volume ≈ 2.4 mL, Cluzeau Info Labo (C.I.L.), Sainte-Foy-La-Grande, France) **(Figure S1)**. Two of these reactors were prepared to fit the UV and the Visible LED irradiation systems. For UV irradiation the tubing was fitted on a metallic grid to allow heat evacuation.

2.3 Syringe pump

The different flow rates of the reactions performed were regulated using a Harvard Apparatus (Holliston, MA, USA) PHD ULTRA XF syringe pump fitted with 8 mL stainless steel syringes (THREAD 1/4 - 28 inch, Ø = 1/16 inch, PC5 702267, Harvard Apparatus).

2.4 LED Systems

Blue (λ = 450 nm) & green (λ = 530 nm) high power spots (50 W electrical power, 4500 lumen, 0.02 $W.cm^{-2}$) LEDs from Bridgelux (Liver-more, CA, USA) were used for the photoinduced ATRP catalyzed by $Ru(bpy)_3Cl_2$ and Eosin Y respectively. Omnicure® AC7300 LEDs of λ = 365 nm and irradiance up to 3 $W.cm^{-2}$ purchased from Lumen Dynamics (Mississauga, Canada) were used for the photoinduced ATRP catalyzed by $CuBr_2$.

3 Methods

3.1 General procedure of ATRP in batch

A Schlenk tube charged with DMF (2 mL, 50% v/v *vs* monomer) and photocatalyst (2 µmol) (for $CuBr_2$, a ligand (TPMA or PMDETA) was added) was sealed with rubber septum and purged with nitrogen during 20 min. Methyl methacrylate (2 mL, 18.8 mmol), that was freshly passed over alumina, EB*i*B (17 µL, 0.1 mmol) and freshly distilled *i*-Pr_2NEt (170 µL, 1 mmol) were then added under nitrogen. The reaction mixture was irradiated with LEDs. UV LEDs (200 $mW.cm^{-2}$, 365 nm) were used for $CuBr_2$/Ligand catalytic system, blue LEDs (50 W, 4500 lumens, 450 nm) for $Ru(bpy)_3Cl_2$ and green LEDs (50 W, 4500 lumens, 530 nm) for Eosin Y. An aliquot was analyzed by ^1H NMR to determine the % of polymerization and by DOSY NMR to determine its M_w. The formed polymer was then precipitated in methanol, filtered and dried under vacuum overnight. A solution of 6 mg/mL in THF was prepared from the dry polymer to be analyzed by GPC.

3.2 General procedure for ATRP in flow

ATRP using the three different catalytic systems with the same composition were performed under flow conditions **(Figure 2, Figure S3)**. The degassed reaction mixture was then transferred into a lab designed FEP tubing reactor (i.d. 800 µm) that was illuminated by LEDs of specific wavelengths depending on the catalytic system **(Figure S1)**.

ATRP using Eosin Y catalyst illuminated by green LEDs in flow

Using the same composition as that in the batch conditions, [MMA]: [initiator]: [Eosin Y]: [*i*-Pr_2NEt] = 200:1:0.02:10 and MMA: DMF= 1:1 (v/v), 4 mL of the reaction mixture was injected within the lab designed microfluidic reactor (FEP tubing, i.d. 800 μm) that was placed in direct contact with the green LEDs. The irradiation time was varied depending on the flow rate that was adjusted by the syringe pump. For each of the two initiators, EBPA and EB*i*B, 6 points that correspond to six different irradiation times were performed. For each point the % of conversion was determined by ^{1}H NMR and the polymers were precipitated, filtered, dried and stored in THF for further analysis by GPC. Note that working under oxygen free conditions was insured, even during the transfer of the reaction mixture from the Schlenk tube to the syringe. The variation of the % of conversion of each polymer *vs* the irradiation time was used to plot the kinetic curves of ATRP in flow.

3.3 Polymers characterization

GPC analysis

Size exclusion chromatography (SEC) was performed at room temperature using a Viscotek GPC max system equipped with a Viscotek guard column (10 × 4.6 mm) and two Viscotek columns LT 5000L mixed medium (300 × 7.8 mm fitted with a Viscotek VE 3580 refractometric detector and a Viscotek VE 3210 UV/Vis detector. THF was used as solvent with a flow rate of 1 mL.min^{-1}. All molecular weights (M_n) and molecular weight distributions (dispersity, M_w/M_n, Đ) were determined by calibration to known, standard poly (methyl methacrylate) samples purchased from Polymer Laboratories (Church Stretton, United Kingdom).

NMR analysis

Proton and carbon magnetic resonance spectra (^{1}H NMR and ^{13}C NMR) were recorded on a Bruker AVANCE 300 spectrometer (^{1}H 300 MHz and ^{13}C 75 MHz) using tetramethylsilane (TMS) as the internal standard. Chemical shifts, δ, are given in ppm and coupling constants, *J*, in Hz. ^{1}H NMR data are reported as follows: chemical shift, multiplicity (s = singlet, d =doublet, t = triplet, dd = doublet of doublets, dt = doublet of triplets, td = triplet of doublets, m = multiplet, brs = broad singlet), coupling constants and integration **(Figure S4)**.

DOSY analysis

DOSY experiments were performed on a Bruker AVANCE 500 spectrometer equipped with an ATMA TXI probe with a z-axis gradient coil. All experiments were run without spinning to avoid convection at temperature of 295 K. Maximum gradient strength was 5.35 G.mm^{-1} and the gradient strengths were varied from 1 to 35 G.cm^{-1}. The standard Bruker pulse program, dstebpgp3s, employing double stimulated echo sequence and 3 spoil gradients was utilized. Bipolar gradients were used with a total duration of 4 ms. Gradient recovery delay was 100 μs, diffusion time was 200 ms and the number of gradient steps was set to be 32. Diffusion coefficients were calculated from T1/T2 analysis module of Topspin 2.1.

Similar to GPC, 2D-NMR is reported to be used for the determination of the weight average molecular mass M_w of the polymer. We run DOSY NMR for PMMA standards of known M_w at 20 °C in $CDCl_3$ instead of benzene-d^6 according to the protocol described by Li and coworkers (Alfredo et al., 2012) Each standard gave a value of diffusion coefficient (*D*) in m^2.s^{-1} whose logarithmic value was plotted as function of the logarithmic value of the corresponding M_w. The calibration curve represented in **Figure 3** was obtained. The plot has an excellent linearity between log *D* *vs* log M_w

with R^2 = 0.999 showing the efficiency of the used protocol. Seven samples of PMMA polymers chosen randomly whose M_w values were determined by GPC were analyzed by DOSY to determine their diffusion coefficients using the same protocol of that of the standards ($CDCl_3$, 20°C). Knowing the value of (D) and by using the equation of the calibration curve log D = -0.4656×log M_w - 7.9116, the M_w values of synthesized PMMA were calculated.

3.4 Preparation of PMMA-Br macroinitiator

In a Schlenk tube, EBPA (17 µL, 0.1 mmol), *i*-Pr_2NEt (170 µL, 1 mmol) and Eosin Y (1.4 mg, 2 µmol) were added to a solution of MMA in DMF (4 mL, 1:1 v/v). The reaction mixture was degassed by three freeze-pump-thaw cycles and pumped through the continuous flow photo-microphotoreactor using a syringe pump connected to the flow reactor *via* a syringe. The solution was pumped through the flow system, at a flow rate of 30 µL.min^{-1} (corresponding to 1 hour of residence time) and irradiated with green LEDs (50 W, 4500 Lumens). The polymer was purified by precipitation in methanol. The resulting macroinitiator was dried overnight, and characterized by GPC.

3.5 Chain extension of PMMA-Br macroinitiator with styrene (St) and Butyl acrylate (BA)

PMMA macroinitiator (0.24 g, 0.02 mmol), *i*-Pr_2NEt (35 µL, 0.2 mmol) and Eosin Y (0.3 mg, 0.43 µmol) were added to a solution of styrene (450 µL, 4 mmol) in 2.5 mL of DMF **(Figure 4)**. The reaction mixture was degassed by three freeze-pump-thaw cycles and pumped through the continuous flow photo-microphotoreactor using a syringe pump connected to the flow reactor *via* a syringe. The solution was pumped through the flow system, at a flow rate of 10 µL.min^{-1} (corresponding to 3 hour of residence time) and irradiated with green LEDs (50 W, 4500 Lumens).The formed copolymer was precipitated, filtered and dried overnight before its analysis by ^{1}H NMR and GPC.

Similarly, copolymerization with butyl acrylate (570 µL, 4 mmol) was performed using the same procedure mentioned above. The formed polymer was then filtered, dried, and analyzed by GPC

3.6 Polymerization of MMA with dark periods

In a Schlenk tube, EBPA (34 µL, 0.2 mmol), *i*-Pr_2NEt (340 µL, 2 mmol) and Eosin Y (2.8 mg, 4 µmol) were added to a solution of MMA in DMF (8 mL, 1:1 v/v). The reaction mixture was degassed by three freeze-pump-thaw cycles and pumped through the continuous flow photo-microphotoreactor using a syringe pump connected to the flow reactor *via* a syringe.

The reaction mixture was irradiated for 3 disrupted hours; after each period of 1 h of irradiation, the solution was kept in dark under argon for 1 h. For every cycle (1 h "LEDs on", 1 h "LEDs off") two samples of 1 mL each were taken for analysis at the beginning and the end of the "LEDs off" period. During the "LEDs on" period, the reaction mixture was pumped through the flow reactor at a flow rate of 30 µL.min^{-1}. Six samples that were taken periodically were precipitated in methanol, filtered and dried overnight for analysis by GPC and NMR.

4 Results and Discussion

4.1 Copper catalyzed ATRP using UV light

First, we optimized the flow protocol. The homemade continuous flow photo-microreactor was made of Fluorinated Ethylene Propylene (FEP) tubing (Ø = 800 µm , L = 1.2 m) that can be easily replaced in case of clogging. FEP is transparent to UV so first we performed a classical ATRP in flow catalyzed by $CuBr_2$ under UV irradiation. Compared to the previously described flow experiment,

UV-LEDs (365 nm) with a power of 200 mW.cm^{-2} were used instead of a medium pressure UV-lamp, and DMSO was replaced by DMF. We also assessed the ligands PMEDTA and TPMA which are commonly used in the literature for Cu catalysed ATRP. Best results were obtained with TPMA **(Table S2, entries 1-8)** leading to 60% conversion and low dispersity ($Đ$ = 1.27) compared to the previous results in flow ($Đ$ = 1.15-1.25).

4.2 Visible light ATRP

We then moved to metallic visible light photoredox catalysis using the $Ru(bpy)_3Cl_2$, *i*-Pr_2NEt system in DMF irradiated by blue LEDs in flow. The modest dispersity **(Table 1, entry 1; $Đ \approx 2$)** obtained is in agreement with the results obtained in batch (Zhang et al., 2011). We then decided to check the activity of Eosin Y, a derivative of fluorescein which is widely used as visible light photoredox catalyst for various organic reactions,(Van Bergen et al., 1979;Hari et al., 2012;Cantillo et al., 2014;Talla et al., 2015) to perform the polymerization of MMA under flow conditions. Eosin Y has its maximum absorption at 539 nm in the visible region of the spectrum and with a high absorption coefficient (ε = 60800 M^{-1} cm^{-1}) **(Figure S6).** The irradiation was afforded by green LEDs with a power of 20 mW.cm^{-2}.

We originally performed polymerization of MMA in DMF using EB*i*B as initiator and Eosin Y as photocatalyst in both batch **(Table 1, entry 2)** and flow **(Table 1, entry 3)**. Interestingly, the change from batch to flow system was enough to improve remarkably both the rate of the reaction and its control. Although 360 min were required in batch to reach a 50% conversion, only 216 min were needed in flow for 70% conversion. Moreover, the dispersity decreased from 1.64 in batch to 1.58 in flow. The results obtained herein in flow are also better than those reported in batch by Yagci group where 120 min of green LEDs irradiation of the reaction mixture gave 28 % conversion but with a dispersity of 1.85 (Kutahya et al., 2016).

Following these results, blank experiments were performed where one of the components (catalyst, initiator, *i*-Pr_2NEt and light) was removed **(Table S3, entry 1)**. In all of these cases no PMMA was detected showing that all of these components are essential for the polymerization process. Moreover, since Eosin Y has a high extinction coefficient, a large amount of the catalyst in flow **(Table 1, entry 4)** will lead to a similar situation to that in batch where the light will only illuminate a small portion of the reactor **(Figure S2, Table S1)**, leading to a decrease in the conversion to 43%. Similarly, decreasing the quantity of Eosin Y will lead to a decrease in the conversion to 50% despite having a better light penetration in the system as the quantity of the catalyst is not efficient to activate the initiators. **(Table 1, entry 5)**. Using EBPA as initiator, which has been previously reported to have a higher activation rate k_{act} compared to EB*i*B due to the radical stability enforced by a phenyl group (Braunecker and Matyjaszewski, 2007), the rate of the polymerization increased remarkably leading to more than 90% of conversion after only 180 min of irradiation **(Table 1, entry 6)**. The polydispersity was also improved to 1.42. To further stabilize the intermediate radical in order to increase the polymerization rate, we used (*p*-OMe)EBPA as initiator; however, the results were quite disappointing **(Table 2, entry 8)**. The tacticity of the obtained polymer was roughly identical whatever the used ATRP conditions **(Table S4, Figure S16)**.

The best conditions obtained for the ATRP initiated by EBPA **(Table 1, entry 6)** were further investigated in details **(Table 2, entries 1-7)**. The polymerization follows a first order kinetics during all the course of the reaction with an equation of $y = 0.123x$ for $ln([MMA]_0/[MMA]_t)$ versus irradiation time (min). The rate constant is 0.123 min^{-1} **(Figure 5, upper panel)** suggesting that the concentration of the propagating radicals is almost constant throughout the polymerization. Molecular weights measured by GPC follow the theoretical values starting from 37% and up to 90%

of conversion suggesting a complete initiation **(Figure 5, lower panel; Table 2, entries 1-7; Figures S9-S14)**. Moderate values of $Đ$ (1.36-1.49) indicate relatively slow deactivation though still in the range of controlled polymerization (< 1.5).

However, note that the first point **(Table 2, entry 1; Figure S9)** does not follow the theoretical M_n so that it deviates upwards in (**Figure 5, Lower panel).** The same results were also observed when using EB*i*B as an initiator **(Figure S8)** which suggests that Eosin Y undergoes an induction period before it can enter the catalytic cycle (Cornils et al., 2020). As a result, this point was excluded from the kinetic analysis **(Figure 5, upper panel).**

4.3 Livingness of the formed polymer

Controlled "on–off" light switching regulation of polymerization was studied by collecting enough polymer after a given period of irradiation and re-injecting it for the next cycle following a 1 hour on / 1 hour off illumination duration. During the LEDs off periods, the polymerization is paused by having dormant alkyl bromides that are protected from any side radical reaction leading to a stagnant conversion and molecular weight; however, these formed polymers are available for reactivation upon re-exposure to light **(Figure 6)**. The polymerization ceased when the light was turned off and started again in response to the irradiation. The control over the formation and termination of active species can be performed by using a simple on-off operation of light leading to M_n *(experimental)* = M_n*(theoretical).*

The "livingness" of the Eosin Y photoinduced ATRP and the termination of the formed polymers by an active bromide ion were further demonstrated by a copolymerization reaction of styrene with a PMMA–Br macroinitiator **(Figure 4)**. The PMMA-Br macroinitiator was firstly synthesized by photoinduced ATRP in flow to get PMMA-Br **(Table 2, entry 7, M_n = 13100, $Đ$ = 1.42)** and then used as a macroinitiator for Eosin Y catalyzed ATRP of styrene (St) and butyl acrylate (BA). The GPC traces of the macroinitiator and the corresponding copolymers are displayed in **Figure 7** and the NMR spectrum of PMMA-*co*-PSt is represented in **Figure S15**. The results of PMMA-*co*-PBA **(Figure 7, red trace)** were not very convenient as the PDI value was 2.1, which signifies a loss in control, that can be attributed with the high reactivity of butyl acrylate that requires strictly anhydrous and oxygen free conditions (Roos et al., 1999). However, the clear shift of M_n of the PMMA-*co*-PSt to a higher molecular weight while still having a good PDI **(Figure 7, blue trace)** and the presence of peaks that correspond to PSt and PMMA in the NMR spectrum indicate an effective copolymerization by re-initiation. These results of PSt copolymerization are in accordance with the literature where clear shifts to lower retention volumes were also reported by performing PMMA chain extension and copolymerization with PSt using the same condition but in batch (Kutahya et al., 2016;Yilmaz and Yagci, 2018).

4.4 Mechanism of Eosin Y catalyzed photoinduced ATRP

The suggested mechanism of the Eosin Y photoinduced electron transfer (PET)-ATRP is represented in **Figure 8**. All the standard potential are in ACN versus SCE Upon irradiation with green LEDs, Eosin Y affords the excited state EY* which has a high oxidation potential (E^0(EY/EY*) = 1.89 V) (Hari and König, 2014). In the activation step, the electron donor, *i*-Pr_2NEt, reductively quenches EY* by a single electron transfer to form a radical anion $EY^{\bullet-}$ and an amine radical cation *i*-$Pr_2N^{\bullet+}Et$ intermediate ($E°$(*i*-Pr_2NEt/*i*-$Pr_2N^{\bullet+}Et$) ≈ 1.0 V). The latter rearranges almost at diffusion rate to the *C*-centered radical *i*-$PrEtNC^{\bullet}(CH_3)_2$ or *i*-$Pr_2NCH^{\bullet}CH_3$ (Wayner et al., 1986;Romero and Nicewicz, 2016). The radical anion $EY^{\bullet-}$ (E^0($EY^{\bullet-}$/EY) = -1.06 V), or the reductive *C*-centered radical (E_0(*C*-centered radical/iminium) = -1.12 V), then transfers an electron to the alkyl bromide EB*i*B or EBPA

(E^0(RX/R$^\bullet$+Br$^-$)= - 0.42 V and -0.20 V respectively) (Lin et al., 2008). The EB*i*B or EBPA radical anion cleaves generating an alkyl radical that adds to the monomer inducing propagation. In the reductive propagation step, the excited Eosin Y recaptures an electron by oxidizing either the bromide ion Br$^-$ into bromine radical Br$^\bullet$ (E^0(Br$^-$/Br$^\bullet$) = 1.75 V) (Isse et al., 2010), or the complex propagating radical, bromide ion by a concerted electron transfer (Pan et al., 2016a). The bromine radical Br$^\bullet$ deactivates the propagation and forms the dormant polymer. The formed radical anion EY$^{\bullet-}$ is reduced to back to EY by providing an electron to the dormant polymer, which has the same structure as a tertiary α-bromoester, that reacts with the monomer. The consumption of the sacrificial amine is to compensate the irreversible terminations of the propagating cycle.

In this mechanism, the very unlikely oxidation of Br$^-$ by the radical cation *i*-Pr$_2$N$^{\bullet+}$Et, (Liu et al., 2016) or the chain radical oxidation to a cation (Xu et al., 2014) are avoided; only a catalytic amount of the sacrificial amine is required to initiate the reaction. Furthermore, all of the steps have favorable redox potentials. This mechanism shows that Eosin Y has a well-established activation deactivation processes that result in the control of the molecular weights and dispersities of the formed polymers.

4.5 Dosy *vs* GPC

Based on the calibration curve obtained using DOSY NMR **(Figure 3)**, M_w values of selected polymers were obtained and presented in **Table 3** along with the corresponding M_w values obtained by GPC. Interestingly, the two methods almost gave the same M_w values in all of the entries. The % of difference between both values varies between 0.08 % in entry 1 to a maximum value of only 5.5 % in entry 7. This shows that DOSY NMR can be a good analytical method for the characterization of polymers. NMR spectroscopy can provide the full characterization of the polymer: % conversion, tacticity, M_n by ^{1}H NMR and M_w by DOSY NMR rendering it complementary to GPC.

5 Conclusion

In conclusion, we have demonstrated that ATRP of MMA using Eosin Y as photocatalyst in a flow reactor illuminated by green LEDs is very efficient affording 90% of conversion in 3 h. Perfect first order kinetics, full initiation or dormant polymer activation, moderate dispersity and masses in agreement with the theoretical values were obtained showing the great mechanistic and synthetic potentials of our conditions. The main reason of this improvement is the homogeneous illumination in flow reactors and hence the shorter reaction time compared to batch (Cambié et al., 2016). We also have shown that NMR spectroscopy (1D and 2D) could be considered as a reliable tool for characterization of polymers. This work combines 3 essential components towards a "greener" chemistry: miniaturization, renewable energy and metal free catalysis that can be used later for scaling up. This work is the first in a series of reactions that our lab is assessing that includes: extending the current continuous-flow system to further improve the irradiation efficiency, synthesizing more complex polymers and using this system for other types of RDRPs.

6 Conflict of Interest

The authors declare that the research was conducted in the absence of any commercial or financial relationships that could be construed as a potential conflict of interest.

7 Author Contributions

All authors listed have made a substantial, direct and intellectual contribution to the work, and approved it for publication.

8 Funding

This work was partially funded by LASeR Association-Lebanon in a form of PhD Scholarship to Nassim El Achi. The NMR and Mass Spectrometry facilities used in this study were funded by the European Community (ERDF), Région Haut de France (France), the CNRS, and the Université de Lille, Faculty of Sciences and Technologies.

9 Acknowledgments

We would like to thank Dr. Benjamin Nottelet and the team at the Institut des Biomolécules Max Mousseron (IBMM) at Université de Monpellier for providing access to the GPC at their facilities.

10 Supplementary Material

The Supplementary Material for this article can be found online at:
https://www.frontiersin.org/articles

11 References

Alfredo, N.V., Jalapa, N.E., Morales, S.L., Ryabov, A.D., Le Lagadec, R., and Alexandrov, L. (2012). Light-Driven Living/Controlled Radical Polymerization of Hydrophobic Monomers Catalyzed by Ruthenium(II) Metalacycles. *Macromolecules* 45**,** 8135-8146.

Anastasaki, A., Nikolaou, V., Zhang, Q., Burns, J., Samanta, S.R., Waldron, C., Haddleton, A.J., Mchale, R., Fox, D., Percec, V., Wilson, P., and Haddleton, D.M. (2014). Copper(II)/Tertiary Amine Synergy in Photoinduced Living Radical Polymerization: Accelerated Synthesis of omega-Functional and alpha,omega-Heterofunctional Poly(acrylates). *J. Am. Chem. Soc.* 136**,** 1141-1149.

Boyer, C., Corrigan, N.A., Jung, K., Nguyen, D., Nguyen, T.K., Adnan, N.N.M., Oliver, S., Shanmugam, S., and Yeow, J. (2016). Copper-Mediated Living Radical Polymerization (Atom Transfer Radical Polymerization and Copper(0) Mediated Polymerization): From Fundamentals to Bioapplications. *Chem. Rev.* 116**,** 1803-1949.

Braunecker, W.A., and Matyjaszewski, K. (2007). Controlled/living radical polymerization: features, developments, and perspectives. *Prog. Polym. Sci.* 32**,** 93-146.

Buss, B.L., and Miyake, G.M. (2018). Photoinduced controlled radical polymerizations performed in flow: methods, products, and opportunities. *Chem. Mater.* 30**,** 3931-3942.

Cambié, D., Bottecchia, C., Straathof, N.J., Hessel, V., and NoëL, T. (2016). Applications of Continuous-Flow Photochemistry in Organic Synthesis, Material Science, and Water Treatment. *Chem. Rev.***,** 10.1021/acs.chemrev.1025b00707.

Cantillo, D., De Frutos, O., RincóN, J.A., Mateos, C., and Kappe, C.O. (2014). Continuous flow α-trifluoromethylation of ketones by metal-free visible light photoredox catalysis. *Org. Lett.* 16**,** 896-899.

Chatani, S., Kloxin, C.J., and Bowman, C.N. (2014). The power of light in polymer science: photochemical processes to manipulate polymer formation, structure, and properties. *Polym. Chem.* 5**,** 2187-2201.

Chen, M., Zhong, M., and Johnson, J.A. (2016). Light-Controlled Radical Polymerization: Mechanisms, Methods, and Applications. *Chem. Rev.* 116**,** 10167-10211.

Chmielarz, P., Fantin, M., Park, S., Isse, A.A., Gennaro, A., Magenau, A.J., Sobkowiak, A., and Matyjaszewski, K. (2017). Electrochemically mediated atom transfer radical polymerization (eATRP). *Prog. Polym. Sci.* 69**,** 47-78.

Cornils, B., Herrmann, W. A., Xu, J. H., & Zanthoff, H. W. (2020). Catalysis from A to Z: a concise encyclopedia. John Wiley & Sons.

Corrigan, N., Almasri, A., Taillades, W., Xu, J., and Boyer, C. (2017). Controlling Molecular Weight Distributions through Photoinduced Flow Polymerization. *Macromolecules* 50**,** 8438-8448.

Corrigan, N., Yeow, J., Judzewitsch, P., Xu, J., and Boyer, C. (2019). Seeing the light: Advancing materials chemistry through photopolymerization. *Angew. Chem. Int. Ed. Engl.* 58**,** 5170-5189.

Discekici, E.H., Anastasaki, A., Read De Alaniz, J., and Hawker, C.J. (2018). Evolution and future directions of metal-free atom transfer radical polymerization. *Macromolecules* 51**,** 7421-7434.

Elliott, L.D., Knowles, J.P., Koovits, P.J., Maskill, K.G., Ralph, M.J., Lejeune, G., Edwards, L.J., Robinson, R.I., Clemens, I.R., Cox, B., Pascoe, D.D., Koch, G., Eberle, M., Berry, M.B., and Booker-Milburn, K.I. (2014). Batch versus Flow Photochemistry: A Revealing Comparison of Yield and Productivity. *Chem. Eur. J.* 20**,** 15226-15232.

Fantin, M., Chmielarz, P., Wang, Y., Lorandi, F., Isse, A.A., Gennaro, A., and Matyjaszewski, K. (2017). Harnessing the interaction between surfactant and hydrophilic catalyst to control e ATRP in miniemulsion. *Macromolecules* 50**,** 3726-3732.

Fors, B.P., and Hawker, C.J. (2012). Control of a Living Radical Polymerization of Methacrylates by Light. *Angew. Chem. Int. Ed. Engl.* 51**,** 8850-8853.

Gao, H., and Matyjaszewski, K. (2006). Synthesis of star polymers by a combination of ATRP and the "click" coupling method. *Macromolecules* 39**,** 4960-4965.

Garlets, Z.J., Nguyen, J.D., and Stephenson, C.R.J. (2014). The Development of Visible-Light Photoredox Catalysis in Flow. *Isr. J. Chem.* 54**,** 351-360.

Hari, D.P., and König, B. (2014). Synthetic applications of eosin Y in photoredox catalysis. *Chem. Commun.* 50**,** 6688-6699.

Hari, D.P., Schroll, P., and KöNig, B. (2012). Metal-free, visible-light-mediated direct C–H arylation of heteroarenes with aryl diazonium salts. *J. Am. Chem. Soc.* 134**,** 2958-2961.

Hu, X., Zhang, Y., Cui, G., Zhu, N., and Guo, K. (2017). Poly (vinylidene fluoride- co- chlorotrifluoroethylene) Modification via Organocatalyzed Atom Transfer Radical Polymerization. *Macromol. Rapid Commun.* 38**,** 1700399.

Hu, X., Zhu, N., Fang, Z., Li, Z., and Guo, K. (2016). Continuous flow copper-mediated reversible deactivation radical polymerizations. *Eur. Polym. J.* 80**,** 177-185.

Isse, A.A., Lin, C.Y., Coote, M.L., and Gennaro, A. (2010). Estimation of standard reduction potentials of halogen atoms and alkyl halides. *J. Phys. Chem. B* 115**,** 678-684.

Konkolewicz, D., Schroder, K., Buback, J., Bernhard, S., and Matyjaszewski, K. (2012). Visible Light and Sunlight Photoinduced ATRP with ppm of Cu Catalyst. *ACS Macro Lett.* 1**,** 1219-1223.

Kutahya, C., Aykac, F.S., Yilmaz, G., and Yagci, Y. (2016). LED and visible light-induced metal free ATRP using reducible dyes in the presence of amines. *Polym. Chem.* 7**,** 6094-6098.

Lin, C.Y., Coote, M.L., Gennaro, A., and Matyjaszewski, K. (2008). Ab initio evaluation of the thermodynamic and electrochemical properties of alkyl halides and radicals and their mechanistic implications for atom transfer radical polymerization. *J. Am. Chem. Soc.* 130**,** 12762-12774.

Liu, X., Zhang, L., Cheng, Z., and Zhu, X. (2016). Metal-free photoinduced electron transfer–atom transfer radical polymerization (PET–ATRP) via a visible light organic photocatalyst. *Polym. Chem.* 7**,** 689-700.

Ma, W.C., Chen, D., Wang, L., Ma, Y.H., Zhao, C.W., and Yang, W.T. (2015). Visible Light-Controlled Radical Polymerization of Propargyl Methacrylate Activated by a Photoredox Catalyst fac- Ir(ppy)(3). *J. Macromol. Sci., Pure Appl. Chem.* 52**,** 761-769.

Ma, W.C., Chen, H.C., Ma, Y.H., Zhao, C.W., and Yang, W.T. (2014). Visible-Light-Induced Controlled Polymerization of Hydrophilic Monomers with Ir(ppy)(3) as a Photoredox Catalyst in Anisole. *Macromol. Chem. Phys.* 215**,** 1012-1021.

Matyjaszewski, K. (2012). Atom Transfer Radical Polymerization (ATRP): Current Status and Future Perspectives. *Macromolecules* 45**,** 4015-4039.

Matyjaszewski, K., and Tsarevsky, N.V. (2009). Nanostructured functional materials prepared by atom transfer radical polymerization. *Nature Chem.* 1**,** 276-288.

Matyjaszewski, K., and Tsarevsky, N.V. (2014). Macromolecular Engineering by Atom Transfer Radical Polymerization. *J. Am. Chem. Soc.* 136**,** 6513-6533.

Matyjaszewski, K., and Xia, J.H. (2001). Atom transfer radical polymerization. *Chem. Rev.* 101**,** 2921-2990.

Melker, A., Fors, B.P., Hawker, C.J., and Poelma, J.E. (2015). Continuous flow synthesis of poly(methyl methacrylate) via a light-mediated controlled radical polymerization. *J. Polym. Sci., Part A: Polym. Chem.* 53**,** 2693-2698.

Miyake, G.M., and Theriot, J.C. (2014). Perylene as an organic photocatalyst for the radical polymerization of functionalized vinyl monomers through oxidative quenching with alkyl bromides and visible light. *Macromolecules* 47**,** 8255-8261.

Mosnacek, J., and Ilcikova, M. (2012). Photochemically Mediated Atom Transfer Radical Polymerization of Methyl Methacrylate Using ppm Amounts of Catalyst. *Macromolecules* 45**,** 5859-5865.

Myers, R.M., Fitzpatrick, D.E., Turner, R.M., and Ley, S.V. (2014). Flow Chemistry Meets Advanced Functional Materials. *Chem. Eur. J.* 20**,** 12348-12366.

Ouchi, M., Terashima, T., and Sawamoto, M. (2008). Precision control of radical polymerization via transition metal catalysis: From dormant species to designed catalysts for precision functional polymers. *Acc. Chem. Res.* 41**,** 1120-1132.

Ouchi, M., Terashima, T., and Sawamoto, M. (2009). Transition Metal-Catalyzed Living Radical Polymerization: Toward Perfection in Catalysis and Precision Polymer Synthesis. *Chem. Rev.* 109**,** 4963-5050.

Pan, X., Fang, C., Fantin, M., Malhotra, N., So, W.Y., Peteanu, L.A., Isse, A.A., Gennaro, A., Liu, P., and Matyjaszewski, K. (2016a). Mechanism of Photoinduced Metal-Free Atom Transfer Radical Polymerization: Experimental and Computational Studies. *J. Am. Chem. Soc.* 138**,** 2411-2425.

Pan, X., Tasdelen, M.A., Laun, J., Junkers, T., Yagci, Y., and Matyjaszewski, K. (2016b). Photomediated Controlled Radical Polymerization. *Prog. Polym. Sci.* 62**,** 73-125.

Pan, X.C., Lamson, M., Yan, J.J., and Matyjaszewski, K. (2015). Photoinduced Metal-Free Atom Transfer Radical Polymerization of Acrylonitrile. *ACS Macro Lett.* 4**,** 192-196.

Priyadarshani, N., Liang, Y.N., Suriboot, J., Bazzi, H.S., and Bergbreiter, D.E. (2013). Recoverable Reusable Polyisobutylene (PIB)-Bound Ruthenium Bipyridine (Ru(PIB-bpy)(3)Cl-2) Photoredox Polymerization Catalysts. *ACS Macro Lett.* 2**,** 571-574.

Ramakers, G., Krivcov, A., Trouillet, V., Welle, A., Möbius, H., and Junkers, T. (2017). Organocatalyzed Photo- Atom Transfer Radical Polymerization of Methacrylic Acid in Continuous Flow and Surface Grafting. *Macromol. Rapid Commun.* 38**,** 1700423.

Ramsey, B.L., Pearson, R.M., Beck, L.R., and Miyake, G.M. (2017). Photoinduced Organocatalyzed Atom Transfer Radical Polymerization Using Continuous Flow. *Macromolecules* 50**,** 2668-2674.

Reis, M.H., Leibfarth, F.A., and Pitet, L.M. (2020). Polymerizations in Continuous Flow: Recent Advances in the Synthesis of Diverse Polymeric Materials. *ACS Macro Lett.* 9**,** 123-133.

Ribelli, T.G., Konkolewicz, D., Bernhard, S., and Matyjaszewski, K. (2014). How are Radicals (Re)Generated in Photochemical ATRP? *J. Am. Chem. Soc.* 136**,** 13303-13312.

Ribelli, T.G., Lorandi, F., Fantin, M., and Matyjaszewski, K. (2019). Atom transfer radical polymerization: billion times more active catalysts and new initiation systems. *Macromol. Rapid Commun.* 40**,** 1800616.

Romero, N.A., and Nicewicz, D.A. (2016). Organic Photoredox Catalysis. *Chem. Rev.***,** 10.1021/acs.chemrev.1026b00057.

Roos, S.G., Müller, A.H., and Matyjaszewski, K. (1999). Copolymerization of n-butyl acrylate with methyl methacrylate and PMMA macromonomers: comparison of reactivity ratios in conventional and atom transfer radical copolymerization. *Macromolecules* 32**,** 8331-8335.

Rubens, M., Latsrisaeng, P., and Junkers, T. (2017). Visible light-induced iniferter polymerization of methacrylates enhanced by continuous flow. *Polym. Chem.* 8**,** 6496-6505.

Ryan, M.D., Pearson, R.M., French, T.A., and Miyake, G.M. (2017). Impact of Light Intensity on Control in Photoinduced Organocatalyzed Atom Transfer Radical Polymerization. *Macromolecules* 50**,** 4616-4622.

Sharma, V., and Tepe, J.J. (2005). Diastereochemical diversity of imidazoline scaffolds via substrate controlled TMSCl mediated cycloaddition of azlactones. *Org. Lett.* 7**,** 5091-5094.

Su, Y.H., Straathof, N.J.W., Hessel, V., and Noel, T. (2014). Photochemical Transformations Accelerated in Continuous-Flow Reactors: Basic Concepts and Applications. *Chem. Eur. J.* 20**,** 10562-10589.

Talla, A., Driessen, B., Straathof, N.J., Milroy, L.G., Brunsveld, L., Hessel, V., and Noel, T. (2015). Metal- Free Photocatalytic Aerobic Oxidation of Thiols to Disulfides in Batch and Continuous- Flow. *Adv. Synth. Catal.* 357**,** 2180-2186.

Tasdelen, M.A., Uygun, M., and Yagci, Y. (2011). Photoinduced Controlled Radical Polymerization. *Macromol. Rapid Commun.* 32**,** 58-62.

Theriot, J.C., Lim, C.H., Yang, H., Ryan, M.D., Musgrave, C.B., and Miyake, G.M. (2016). Organocatalyzed atom transfer radical polymerization driven by visible light. *Science* 352**,** 1082-1086.

Tonhauser, C., Nataello, A., Lowe, H., and Frey, H. (2012). Microflow Technology in Polymer Synthesis. *Macromolecules* 45**,** 9551-9570.

Treat, N.J., Fors, B.P., Kramer, J.W., Christianson, M., Chiu, C.Y., De Alaniz, J.R., and Hawker, C.J. (2014a). Controlled Radical Polymerization of Acrylates Regulated by Visible Light. *ACS Macro Lett.* 3**,** 580-584.

Treat, N.J., Sprafke, H., Kramer, J.W., Clark, P.G., Barton, B.E., Read De Alaniz, J., Fors, B.P., and Hawker, C.J. (2014b). Metal-free atom transfer radical polymerization. *J. Am. Chem. Soc.* 136**,** 16096-16101.

Van Bergen, T., Hedstrand, D.M., Kruizinga, W.H., and Kellogg, R.M. (1979). Chemistry of dihydropyridines. 9. Hydride transfer from 1, 4-dihydropyridines to sp3-hybridized carbon in sulfonium salts and activated halides. Studies with NAD (P) H models. *J. Org. Chem.* 44**,** 4953-4962.

Wayner, D.D., Dannenberg, J.J., and Griller, D. (1986). Oxidation potentials of α-aminoalkyl radicals: bond dissociation energies for related radical cations. *Chem. Phys. Lett.* 131**,** 189-191.

Wenn, B., Conradi, M., Carreiras, A.D., Haddleton, D.M., and Junkers, T. (2014). Photo-induced copper-mediated polymerization of methyl acrylate in continuous flow reactors. *Polym. Chem.* 5**,** 3053-3060.

Xu, J.T., Atme, A., Martins, A.F.M., Jung, K., and Boyer, C. (2014). Photoredox catalyst-mediated atom transfer radical addition for polymer functionalization under visible light. *Polym. Chem.* 5**,** 3321-3325.

Yang, Q.Z., Dumur, F., Morlet-Savary, F., Poly, J., and Lalevee, J. (2015). Photocatalyzed Cu-Based ATRP Involving an Oxidative Quenching Mechanism under Visible Light. *Macromolecules* 48**,** 1972-1980.

Yilmaz, G., and Yagci, Y. (2018). Photoinduced metal-free atom transfer radical polymerizations: state-of-the-art, mechanistic aspects and applications. *Polym. Chem.* 9**,** 1757-1762.

Zhang, C., Wang, L., Jia, D., Yan, J., and Li, H. (2019). Microfluidically mediated atom-transfer radical polymerization. *Chem. Commun.* 55**,** 7554-7557.

Zhang, G., Song, I.Y., Ahn, K.H., Park, T., and Choi, W. (2011). Free Radical Polymerization Initiated and Controlled by Visible Light Photocatalysis at Ambient Temperature. *Macromolecules* 44**,** 7594-7599.

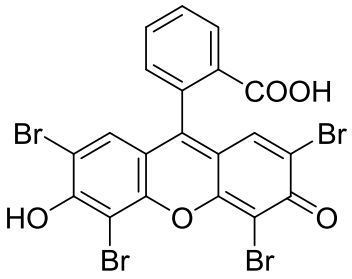

Figure 1. Structure of Eosin Y

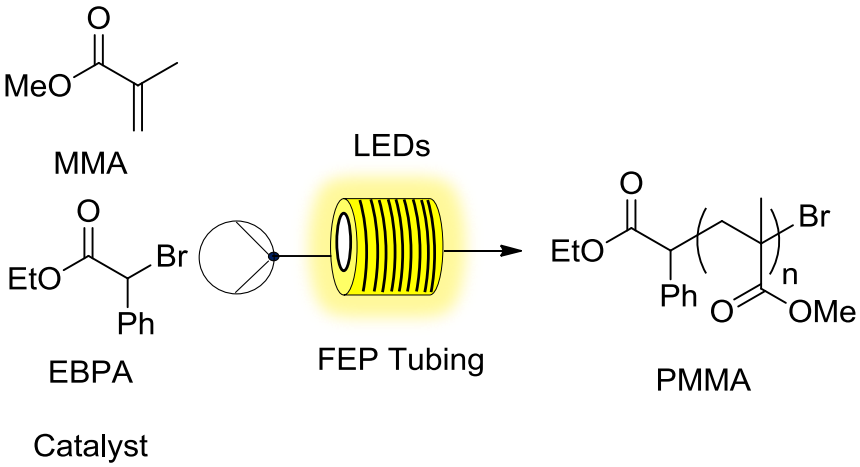

Figure 2. Polymerization systems studied in flow

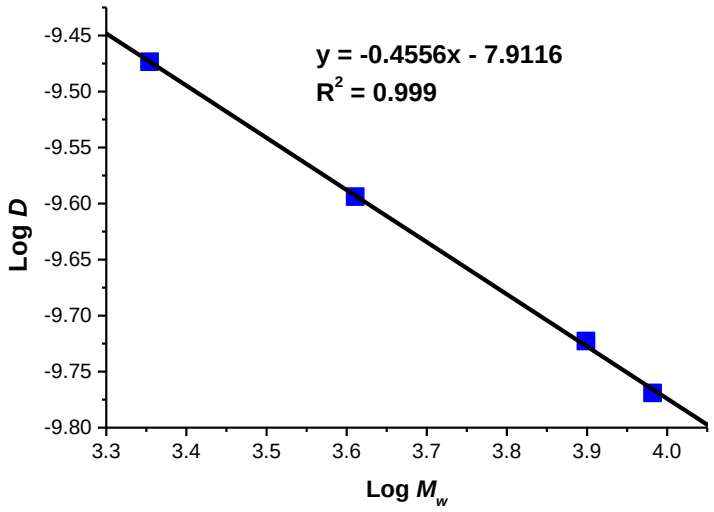

Figure 3. PMMA calibration curve in $CDCl_3$ used for determining M_w by DOSY NMR

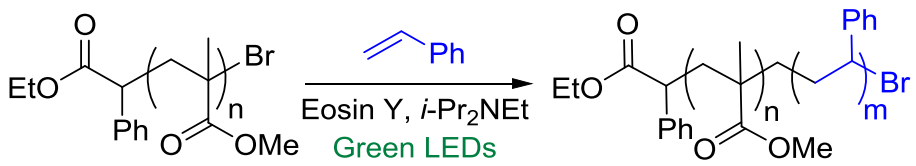

Figure 4. PMMA-Br copolymerization with styrene using Eosin Y in flow

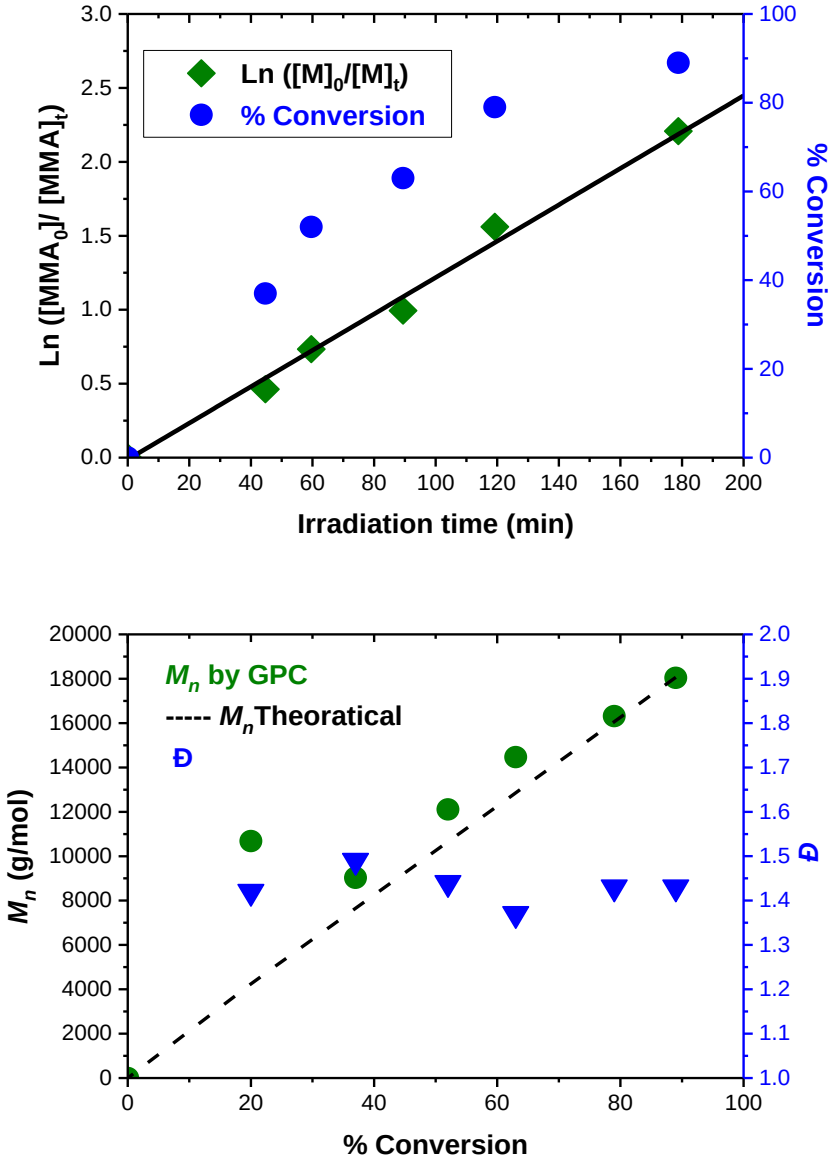

Figure 5. MMA polymerization catalyzed by Eosin Y using EBPA as initiator. (Upper panel) kinetics of MMA consumption providing an equation of *y= 0.123x* for ln([MMA]0/[MMA]t) versus irradiation time (min). (Lower panel) PMMA M_n measured by GPC (left scale) and dispersity (right scale)

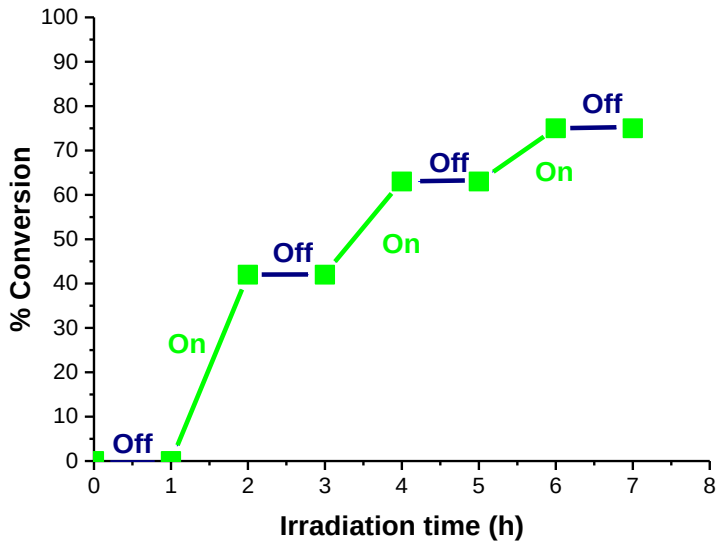

Figure 6. On-off MMA polymerization catalyzed by Eosin Y using EBPA as initiator

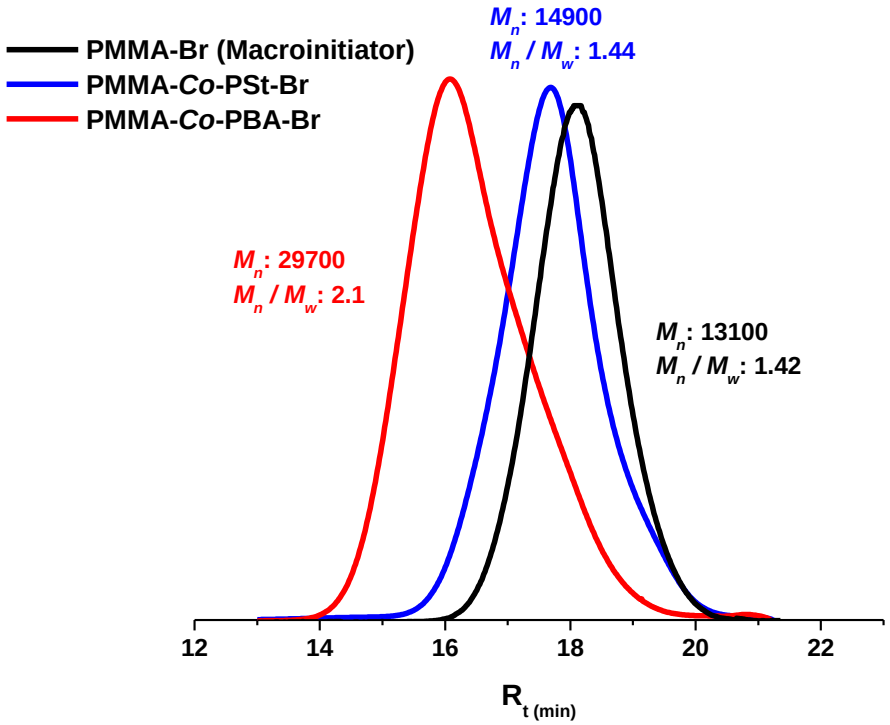

Figure 7. Block polymer synthesis. GPC traces of PMMA (black), PMMA-*co*- PSt (blue) and PMMA-*co*- PBA (red) block polymers

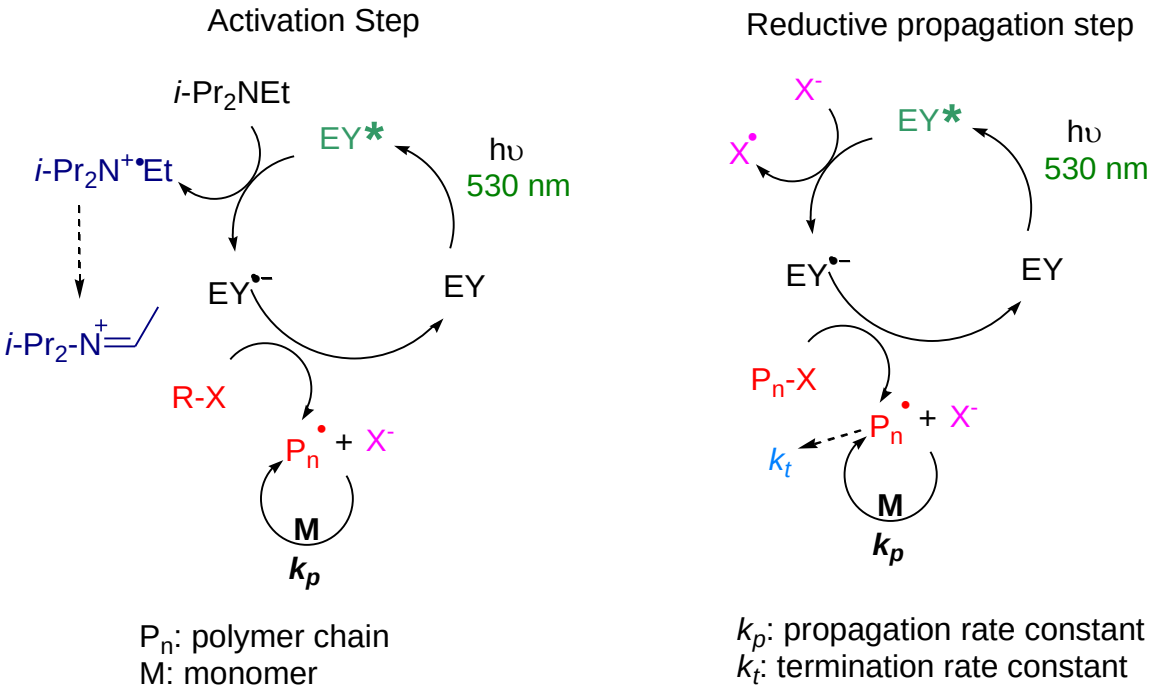

Figure 8. Suggested photoinduced electron transfer ATRP mechanism by Eosin Y / *i*-Pr_2NEt catalyst

573 **Table 1** ATRP polymerization of MMA in DMF in a flow microreactor using LEDs irradiation[a]

Entry	Catalyst	Initiator / Additive	Polymerization conditions[a]	LEDs	Conv. (%)[b]	Time (min)	M_n theo[c]	M_n[d]	$Đ$[d]
1	$Ru(bpy)_3Cl_2$	EB*i*B / *i*-Pr_2NEt	200:1:0.01:10	blue	86	430	17200	20600	1.96
2[e]	Eosin Y	EB*i*B / *i*-Pr_2NEt	200:1:0.01:10	green	54	360	11000	24300	1.64
3	Eosin Y	EB*i*B / *i*-Pr_2NEt	200:1:0.01:10	green	70	216	14000	25000	1.58
4	Eosin Y	EB*i*B / *i*-Pr_2NEt	200:1:0.05:10	green	43	216	8600	18000	1.86
5	Eosin Y	EB*i*B / *i*-Pr_2NEt	200:1:0.003:10	green	50	216	10000	17600	1.85
6	Eosin Y	EBPA /*i*-Pr_2NEt	200:1:0.01:10	green	91	180	18000	18000	1.42

574 [a]Polymerization conditions: [MMA]: [Initiator]: [Catalyst]:[Additive] = 200:1:x:y in DMF at RT in a
575 microreactor illuminated with LEDs. [b]Determined by ^{1}H NMR. [c]$M_{n\ theo}$= ([MMA]/ [Initiator] × conv.
576 × M_{MMA}) + $M_{Initiator}$. [d]Determined by GPC. [e]Performed in batch

577

578 **Table 2**. Eosin Y catalyzed ATRP of MMA using EBPA as an initiator in flow[a]

Entry	Time (min)	% Conv.[b]	M_n theo[c]	M_n by GPC	$Đ$[d]
1	36	20	4280	10400	1.46
2	45	37	7650	9040	1.49
3	60	52	10650	12050	1.44
4	90	63	12860	13050	1.36
5	120	79	16060	16350	1.43
6	180	89	18060	18250	1.41
7[e]	60	53	10650	13000	1.42
8[f]	360	54	11100	24280	1.64
9[g]	180	70	14290	19500	1.46

579 [a]Polymerization conditions: [MMA]: [EB*PA*]: [Eosin Y]: [*i*-Pr_2NEt] = 200:1:0.02:10 in DMF at RT
580 in microreactor illuminated with green LEDs. [b]Determined by ^{1}H NMR. [c]M_n theo= ([MMA]/[EB*PA*]
581 × conversion × M_{MMA}) + $M_{EBPA;}$ where [MMA] and [EBPA] are the concentrations of the monomer
582 and the initiator respectively and M_{MMA} and M_{EBPA} are their corresponding molar masses.
583 [d]Determined by GPC. [e]Used for copolymerization with styrene. [f]Performed in batch. [g]Using *p*(OMe)-
584 EBPA synthesized according to the procedure listed by Sharma and Tepe (Sharma and Tepe, 2005).

585

Table 3. M_w of PMMA synthesized in flow by DOSY NMR and GPC

Entry	$D \times 10^{-10}$ by DOSY ($m^2.s^{-1}$)	M_w by DOSY[a]	M_w by GPC.	% diff [b]
1	1.10	24920	24900	0.08
2	1.20	20740	20270	2.32
3	1.25	19100	19150	-0.26
4	1.26	18710	18040	3.70
5	1.28	18020	17980	0.22
6	1.30	17550	17290	1.50
7	1.96	7190	6810	5.58

586 [a] Equation of the PMMA standard calibration curve is log D = -0.4656 log M_w - 7.9116 was used to
587 determine M_w using the values of D provided by DOSY NMR. [b] Calculated from M_w (GPC) and
588 M_w (DOSY).

589